Hot nucleons in chiral soliton models

H. Walliser
Fachbereich Physik, Universität-GH-Siegen, D-57068 Siegen, Germany
(Received 28 April 1997)

Nucleons in a hot pion gas are studied within the framework of chiral soliton models which contain pions and also baryons as solitons of the same chiral action. The semiclassical treatment of the soliton solutions must be augmented by pionic fluctuations which requires renormalization to one loop, and finite temperatures do not introduce new ultraviolet divergencies and may easily be considered. Alternatively, a renormalization scheme based on the renormalization group equation at finite temperature comprises and extends the rigorous results of chiral perturbation theory and renders the low-energy constants temperature dependent, which allows the construction of temperature-dependent solitons below the critical temperature. The temperature dependence of the baryon energy and the pion-nucleon coupling is studied. There is no simple scaling law for the temperature dependence of these quantities. [S0556-2821(97)05519-7]

PACS number(s): 11.10.Wx, 12.39.Dc, 12.39.Fe

I. INTRODUCTION

It is generally believed that with increasing temperature hadronic matter undergoes a phase transition to a quark gluon plasma which hopefully might be produced in heavy-ion collisions. Already below the critical temperature we expect the baryon properties to change; of particular interest are variations in the nucleon mass M and the pion-nucleon coupling constant $g_{\pi NN}$, which determine the behavior of hot nucleonic matter.

Eletsky and Kogan [1] use chiral perturbation theory (ChPT) to show that the temperature dependence of the axial-vector coupling constant g_A turns out to be the same as for the pion decay constant f_π. With the assumption that the baryon mass is temperature-independent and with the Goldberger-Treiman relation $f_\pi g_{\pi NN}=Mg_A$ they obtain

$$M\sim 1, \quad g_A\sim f_\pi, \quad g_{\pi NN}\sim 1, \tag{1.1}$$

a pion-nucleon coupling which remains essentially unchanged.

Bernard and Meissner [2] use a chiral soliton model with explicit vector mesons together with a temperature-dependent f_π lent from ChPT [3] or from the Nambu–Jona-Lasinio (NJL) model [4]. Qualitatively their results may be understood by the simple scaling

$$M\sim f_\pi, \quad g_A\sim g_{\pi NN}\sim 1, \tag{1.2}$$

which in tree approximation becomes exact in a pure Skyrme model (without pion mass term) and which is at variance with Eq. (1.1) although with the same result of a temperature-independent pion-nucleon coupling.

The simple relations (1.2) applied to the density dependence of these quantities have nowadays come to be known as Brown-Rho scaling [5]. We do not want to discuss here what happens if the density is varied, but concerning the temperature there are definitely no reasons that these relations should hold. Namely, the temperature dependence is carried by the one-loop contribution which does not scale as the tree approximation (Sec. II). Even if the renormalization is performed at finite temperature such that the low-energy constants (LEC's) in the effective action (in particular the pion decay constant) and hence also the tree approximation become temperature dependent, the remaining one-loop contribution, which cannot be omitted, destroys these simple scaling relations (Sec. III).

II. ONE-LOOP AT FINITE TEMPERATURE

The starting point of our investigation is the standard chiral Lagrangian as given by Gasser and Leutwyler [6]:

$$\begin{aligned}\mathcal{L}(U)&=\frac{f^2}{2}[\boldsymbol{\alpha}_\mu\boldsymbol{\alpha}_\mu-2m^2u]+\ell_2(\boldsymbol{\alpha}_\mu\times\boldsymbol{\alpha}_\nu)^2\\&\quad-(\ell_1+\ell_2)(\boldsymbol{\alpha}_\mu\boldsymbol{\alpha}_\mu)^2+\ell_4m^2(\boldsymbol{\alpha}_\mu\boldsymbol{\alpha}_\mu)u\\&\quad-(\ell_3+\ell_4)m^4u^2+\cdots\\&=\frac{f^2}{2}\boldsymbol{\alpha}_\mu\boldsymbol{\alpha}_\mu-f^2m^2u+\sum_i^4\ell_i\mathcal{L}_i^{(4)}+\cdots,\end{aligned} \tag{2.1}$$

with the abbreviations

$$U^\dagger D_\mu U\equiv i\boldsymbol{\tau}\cdot\boldsymbol{\alpha}_\mu, \quad \tfrac{1}{4}\mathrm{tr}(U+U^\dagger)\equiv u, \quad U\in \mathrm{SU}(2).$$

The first term in Eq. (2.1) represents the nonlinear σ model (NLSM) which is of chiral order 2 [Ch$O(2)$] followed by the relevant Ch$O(4)$ terms. For the time being the LEC's take their standard values at scale $\mu=m_\rho$ in order to guarantee that the Lagrangian be leading order in the number of colors N_C. In the following we intend to use the same effective action in the vacuum sector and in the soliton sector; the necessary modifications will be discussed immediately. For the description of one-loop effects fluctuations $\boldsymbol{\eta}$,

$$U=A\sqrt{U_0}\exp(i\boldsymbol{\tau}\boldsymbol{\eta}/f)\sqrt{U_0}A^\dagger, \tag{2.2}$$

are introduced around the classical solution U_0:

$$\begin{aligned}U_0&=1, \quad \text{vacuum sector},\\U_0&=\exp[i\boldsymbol{\tau}\hat{\mathbf{r}}F(r)], \quad \text{soliton sector}\end{aligned} \tag{2.3}$$

which, in the soliton sector, is of the familiar hedgehog type. Rotational degrees of freedom are considered in the Euler angle-dependent SU(2) rotation matrix A; translations are unimportant in this context. The different classical solutions in the two sectors lead to decisive implications for the proper one-loop treatment: while in the vacuum sector perturbation theory (ChPT) applies as far as the external momenta are kept small; the soliton sector's Casimir energy has to be evaluated via the phase shifts generated by the scattering equations for the fluctuations which sum the one-loop contribution to *all* chiral orders. This complication is caused by the gradients of the chiral profile in Eq. (2.3) which are of the order m_ρ and not small.

For the same reason, in the soliton sector the higher chiral order terms in the Lagrangian (2.1) are important and may not simply be neglected. The most elegant way to add higher chiral orders to the effective action proceeds through the coupling of vector mesons which leave the Lagrangian to Ch$O(4)$ untouched. However, unfortunately vector mesons come along with numerous technical difficulties (many more degrees of freedom, induced components, etc.) whose proper treatment becomes very complicated. The most simple alternative is to use an *effective* LEC $\ell_2 = 1/4e^2$ in front of the Skyrme term. The choice $e = 4.25$ (instead of $e = 7.24$) simulates the higher chiral order terms generated by vector mesons [7]. Tree contributions to soliton mass and radius of the standard Ch$O(4)$ lagrangian with and without effective Skyrme parameter are compared with typical vector meson results in Table I. For $e = 7.24$ the tree mass of 940 MeV is reduced to 385 MeV if one-loop corrections are included. This soliton is just too small. With the effective Skyrme parameter $e = 4.25$ the tree values are of the typical magnitude obtained also from vector meson models. For a more detailed justification of this choice see Ref. [7].

Observables other than the mass may be calculated by coupling to the corresponding external fields. External electromagnetic and axial fields couple through the covariant derivative D_μ and the external scalar field, relevant for quark condensate and σ term, couples to the quark mass contained in the parameter m^2. In general the external field j with strength ε adds to the Lagrangian in the form

$$\mathcal{L}(\varepsilon) = \mathcal{L}(\ell_i, U) - \varepsilon j \cdot J(\ell_i, U), \tag{2.4}$$

where $J(\ell_i, U)$ denotes the corresponding current density. The external field has to be chosen suitably so as to give the desired quantity, for details see Ref. [7]. Matrix elements of $j \cdot J$ are then obtained as a derivative of the soliton mass (tree + one loop) in the presence of the external field with respect to its strength.

TABLE I. Tree contribution to the soliton mass and the baryon radius for the Ch$O(4)$ Lagrangian with LEC's at scale $\mu = m_\rho$ ($e = 7.24$) and for the same Lagrangian with an effective Skyrme parameter $e = 4.25$, compared with typical vector meson results (see e.g., [8]).

	Soliton mass M [MeV]	Baryon radius $\langle r^2 \rangle_B$ [fm^2]
Ch$O(4)$ Lagrangian ($e = 7.24$)	940	0.09
Effective Skyrme term $e = 4.25$	1630	0.24
Vector meson Lagrangian	$\simeq$ 1500–1600	$\simeq$ 0.2–0.3

Later on all thermodynamical quantities of the vacuum and soliton sector, respectively, such as thermodynamical potentials, entropy, and so on are derived from the partition functions ($\beta = T^{-1}$)

$$\ln Z_{\rm vac} = \beta V \left[f^2 m^2 + \frac{3}{2} g_0(m,T) \right],$$

$$\ln Z = \ln Z_{\rm vac} - \beta M - \beta F_{\rm Cas}. \tag{2.5}$$

The vacuum partition function comprises the tree contribution $f^2 m^2$ of the Lagrangian (2.1) with $U_0 = 1$ and the familiar one-loop contribution for free massive pions $\frac{3}{2} g_0(m,T)$ (2.16). Analogously, in the soliton sector there appears the soliton mass M in tree approximation and the temperature dependence resides for the time being in the free Casimir energy $F_{\rm Cas}$ (one-loop contribution) which is generated by the fluctuations off the soliton background. The corresponding equations of motion for the fluctuatons (2.2) are solved for the phase shifts in the intrinsic frame. Because these equations decouple into partial waves characterized by phonon spin L and parity the phase shifts may be calculated individually and summed up over the various channels (Lc):

$$\delta(p) = \sum_{Lc} (2L+1)\, \delta_{Lc}(p). \tag{2.6}$$

Technically, this calculation is quite involved and the reader is refered to [7] for details. With the phase shifts (2.6) the Casimir energy may be evaluated by means of the formula [9]

$$\begin{aligned} F_{\rm Cas} &= \frac{1}{\pi} \int_0^\infty dp\, \delta'(p) \left[\frac{\omega}{2} + \frac{1}{\beta} \ln(1 - e^{-\beta\omega}) \right] \\ &= -\frac{1}{\pi} \int_0^\infty dp \frac{p}{\omega} \delta(p) \left[\frac{1}{2} + \frac{1}{e^{\beta\omega} - 1} \right] \\ &\quad - \frac{\delta(0)}{\pi} \left[\frac{m}{2} + \frac{1}{\beta} \ln(1 - e^{-\beta m}) \right]. \end{aligned} \tag{2.7}$$

This expression is ultraviolet divergent and requires renormalization. It should be noticed here that the divergence is located in the temperature-independent part, the temperature-dependent part is perfectly finite and does not introduce new infinities [see Eq. (2.15) below]. The divergencies are related to the high momentum behavior of the phase shifts:

$$\delta(p) \underset{p \to \infty}{\sim} a_0 p^3 + a_1 p + \frac{a_2}{p} + \cdots \tag{2.8}$$

(the denoted terms give rise to at least logarithmically divergent expressions). The constants a_0, a_1, and a_2 are related to the corresponding heat kernels and are known analytically for the NLS model [first term in Eq. (2.1)]:

$$a_0=0,$$

$$a_1=\frac{1}{4\pi}\int d^3r[2\boldsymbol{\alpha}_\mu\boldsymbol{\alpha}_\mu-3m^2(u-1)], \tag{2.9}$$

$$a_2=\frac{1}{8\pi}\int d^3r[\tfrac{1}{3}(\boldsymbol{\alpha}_\mu\boldsymbol{\alpha}_\mu)^2+\tfrac{2}{3}(\boldsymbol{\alpha}_\mu\boldsymbol{\alpha}_\nu)^2 -2m^2(\boldsymbol{\alpha}_\mu\boldsymbol{\alpha}_\mu)(u-1)+\tfrac{3}{2}m^4(u-1)^2].$$

Values for the full model (2.1) $a_0=0.1m_\pi^{-3}$, $a_1=3.6m_\pi^{-1}$, and $a_2=15.2m_\pi$ have to be determined numerically and the phase shifts are needed with great precision up to $p_{\max}\simeq 25m_\pi$ where $L_{\max}\simeq 100$ partial waves are needed [7]. The strategy is now to subtract the troublesome terms in the phase shift integral and add them separately using dimensional regularization which involves a scale μ hidden in λ, G_0, G_1, and G_2:

$$F_{\rm Cas}=-\frac{1}{\pi}\int_0^\infty dp\frac{p}{\omega}\left[\delta(p)-a_0p^3-a_1p-\frac{a_2}{p}\right]\left[\frac{1}{2}+\frac{1}{e^{\beta\omega}-1}\right] -\frac{\delta(0)}{\pi}\left[\frac{m}{2}+\frac{1}{\beta}\ln(1-e^{-\beta m})\right] +\lambda[3\pi m^4a_0-4\pi m^2a_1+8\pi a_2] -3\pi a_0G_0-2\pi a_1G_1-4\pi a_2G_2. \tag{2.10}$$

The pole contributions $(d\to 4)$ located in

$$\lambda=\frac{\mu^{d-4}}{16\pi^2}\left[\frac{1}{d-4}-\frac{1}{2}[\Gamma'(1)+\ln(4\pi)+1]\right] \tag{2.11}$$

may be renormalized

$$3\pi m^4a_0-4\pi m^2a_1+8\pi a_2=\sum_i\gamma_i\int d^3r\mathcal{L}_i^{(4)}+\cdots \tag{2.12}$$

into the Ch$O(\geqslant 4)$ terms of the Lagrangian. In Ch$O(4)$ the coefficients γ_i [6] are simple numerical factors and the pole contributions are absorbed in the renormalized LEC's $\ell_i\to\ell_i+\gamma_i\lambda$ just as in standard ChPT. The remaining expression for the Casimir energy

$$F_{\rm Cas}=-\frac{1}{\pi}\int_0^\infty dp\frac{p}{\omega}\left[\delta(p)-a_0p^3-a_1p-\frac{a_2}{p}\right]\left[\frac{1}{2}+\frac{1}{e^{\beta\omega}-1}\right] -\frac{\delta(0)}{\pi}\left[\frac{m}{2}+\frac{1}{\beta}\ln(1-e^{-\beta m})\right] -3\pi a_0G_0-2\pi a_1G_1-4\pi a_2G_2 \tag{2.13}$$

is finite: it is the central formula of our formulation. The explicit temperature and scale-dependence is contained in the contributions

$$G_0=g_0(m,T)-\frac{m^4}{32\pi^2}\left(\frac{1}{6}+\ln\frac{m^2}{\mu^2}\right),$$

$$G_1=g_1(m,T)+\frac{m^2}{16\pi^2}\ln\frac{m^2}{\mu^2}, \tag{2.14}$$

$$G_2=g_2(m,T)-\frac{1}{16\pi^2}\left(1+\ln\frac{m^2}{\mu^2}\right).$$

Let us postpone the discussion of the temperature dependence together with the definition of the heat functions $g_\nu(m,T)$ for a moment. The explicit scale dependence in Eq. (2.14) should be compensated for by the scale dependent LEC's. This is actually the case also in the soliton sector: at $T=0$ the LEC's introduce a scale dependence to the soliton in tree approximation. This scale dependence is compensated for by the one-loop contribution such that the mass and other baryon properties remain independent from the scale μ over a wide region (Figs. 3.2 and 3.3 in Ref. [7]). Towards smaller values then ($\mu\simeq 420$ MeV) the symmetric Ch$O(4)$ term $(\boldsymbol{\alpha}_\mu\boldsymbol{\alpha}_\mu)^2$ in the Lagrangian (2.1) becomes too strong and finally destroys the soliton. The renormalization scheme relies on the premises of the existence of such a scale region with almost constant baryon properties which therefore supports the reasonable choice for the effective Skyrme parameter $e=4.25$. For the standard ChPT value $e=7.24$ there appears a severe scale dependence. Typical tree and one-loop values for several observables (mass M, sigma term σ, axial-vector coupling g_A, isovector magnetic moment μ_V, and electric polarizability α) are given in Table II. The one-loop contributions generally improve the tree values towards the experimental data except for the axial-vector quantities. Because of the Adler-Weissberger relation $g_A^2=1+\cdots$ a large $1/N_C$ contribution to g_A is expected [7]. This unpleasant fea-

TABLE II. Tree and tree + one-loop values for some typical observables considered for the model with effective Skyrme parameter $e=4.25$. For the axial coupling constant a $1/N_C$ piece estimated from current algebra is added.

	tree $O(N_C)$	tree + one-loop $O(N_C)+O(1)$	tree + one-loop + CA correction	experiment
M [MeV]	1630	946		938
σ [MeV]	54	33		45 ± 7
g_A	0.91	0.66	1.20	1.26
μ^V	1.62	2.24		2.35
α [10^{-4} fm^3]	17.8	9.8		9.5 ± 5

ture caused by the algebra of the axial currents which mixes different N_C orders is common to all models relying on the $1/N_C$ expansion.

The temperature dependence of the free Casimir energy (2.13) and of the internal Casimir energy is made explicit by writing

$$F_{\rm Cas}(T)=F_{\rm Cas}(0)+\frac{1}{\pi\beta}\int_0^\infty dp\,\delta'(p)\ln(1-e^{-\beta\omega}),$$

$$U_{\rm Cas}(T)=F_{\rm Cas}(T)-T\frac{\partial F_{\rm Cas}(T)}{\partial T}$$

$$=U_{\rm Cas}(0)+\frac{1}{\pi}\int_0^\infty dp\frac{\omega\,\delta'(p)}{e^{\beta\omega}-1}. \qquad (2.15)$$

As already mentioned the temperature-dependent part is finite and requires no extra renormalization. The important contributions come from the terms proportional to the heat functions contained in the terms G_0, G_1, G_2 [last column in Eq. (2.13)]

$$g_0(m,T)=\frac{2}{3(2\pi)^3}\int d^3p\frac{p^2}{\omega}\frac{1}{e^{\beta\omega}-1}$$

$$\overset{T\gg m}{=}\frac{\pi^2}{45}T^4-\frac{m^2T^2}{12}+\frac{m^3T}{6\pi}+\cdots, \qquad (2.16)$$

$$g_1(m,T)=\frac{1}{(2\pi)^3}\int d^3p\frac{1}{\omega}\frac{1}{e^{\beta\omega}-1}\overset{T\gg m}{=}\frac{T^2}{12}-\frac{mT}{4\pi}+\cdots,$$

$$g_2(m,T)=\frac{1}{2(2\pi)^3}\int d^3p\frac{1}{p^2\omega}\frac{1}{e^{\beta\omega}-1}\overset{T\gg m}{=}\frac{T}{8\pi m}+\cdots,$$

which are of Ch$O(4)$, Ch$O(2)$, and Ch$O(0)$, respectively. Although we could have integrated (2.15) directly, we use Eqs. (2.13), (2.14) with the heat functions (2.16) to make the connection to the renormalization at finite temperature (next section) more transparent.

The temperature-independent tree and the temperature-dependent one-loop contributions to the free and internal soliton energies

$$F_{\rm sol}\equiv-\frac{\ln Z/Z_{\rm vac}}{\beta}=M+F_{\rm Cas},$$

$$U_{\rm sol}\equiv-\frac{\partial\ln Z/Z_{\rm vac}}{\partial\beta}=M+U_{\rm Cas}, \qquad (2.17)$$

are plotted in Fig. 3 (dashed lines). By construction this energy definition yields a thermal mass shift that is always real. Since at finite temperature the Poincaré symmetry is violated alternative definitions of the mass shift via the recoil mass or through the thermal propagator [10] do not necessarily lead to the same result. For instance the latter definition generally leads to a complex pole mass which reflects particle absorption and the nucleon's damping. The choice is process dependent and the energy mass definition used here captures the essentials of the bulk state properties and is also suitable to calculate other baryon properties. The issue is discussed in [11] for $(1+1)$-dimensional models.

Both energies $F_{\rm sol}$ and $U_{\rm sol}$ remain almost constant over the low-temperature region. Towards the critical temperature $F_{\rm sol}$ decreases and $U_{\rm sol}$ increases as expected, but there we cannot trust the one-loop approximation (next section). The different behavior of free and internal energies is not surprising: this is observed already for massless bosons in the vacuum [compare also Eq. (3.7)]. The behavior of the axial coupling g_A shown in Fig. 4 (dashed line) is more sensitive: it decreases with increasing temperature already at relatively low temperatures.

In the chiral limit $m\to 0$ the soliton-meson interaction vanishes at low momenta $\delta'(p)=b_0p^2+O(p^4)$ and the Casimir energy (2.15) remains perfectly well defined. In this limit we obtain for low temperatures a mass shift $U_{\rm sol}(T)=U_{\rm sol}(0)+b_0(\pi^3/15)T^4$ in accordance with a general theorem which states that there is no contribution of order T^2.

The temperature dependence by expection of Eq. (2.15) is nontrivial. Therefore in the following section we perform the renormalization at finite temperature in order to obtain a temperature-dependent soliton (tree approximation). Because the scaling (1.2) of the tree approximation is simple one might expect a similar behavior for the total temperature-dependent contribution. This expection will prove wrong.

III. RENORMALIZATION GROUP AT FINITE TEMPERATURE

Because the temperature-dependent contribution to the Casimir energy is finite there is of course some ambiguity in setting up the renormalization scheme. Among the three relevant terms in the Casimir energy (2.13), the first one proportional to a_0 is of higher chiral order [at least Ch$O(6)$] and numerically small. For the remaining terms proportional to a_1 and a_2 there are several possibilities

(i) No renormalization: both terms are kept in the one-loop contribution, the renormalized LEC's take their values at $T=0$. This was the choice made in Sec. II.

(ii) Minimal renormalization: the a_1 term is renormalized into the NLS model [first term in Eq. (2.1)] and renders the parameters f and m temperature dependent. The a_2 term is kept in the one-loop contribution, the Ch$O(4)$ LEC's $\ell_i(\mu)$ are untouched and remain at their $T=0$ values. The resulting temperature dependence of f and m will prove to be in accordance with the expectations of ChPT.

(iii) Maximal renormalization: both the a_1 and the a_2 term are renormalized into the NLS model and the Ch$O(4)$ piece of the Lagrangian, respectively. Because in the original Lagrangian there are no other terms this corresponds to a maximal renormalization of the temperature-dependent one-loop. Now the ℓ_i's also become temperature dependent:

$$\ell_i(\mu,T)=\ell_i(\mu)+\frac{\gamma_i}{2}g_2(m,T)$$

through the heat function $g_2(m,T)$. Unfortunately this function diverges in the chiral limit $m\to 0$ [compare Eq. (2.16)] and hence also the renormalized ℓ_i's, leading to an ill-defined Lagrangian. Thus, in this renormalization scheme the

total finite temperature-dependent contribution (2.15) is artificially split into infinite tree and one-loop contributions for vanishing pion mass, which is very unpleasant.

There is another unpleasant feature of the maximal renormalization scheme: because the coefficient $\ell_1+\ell_2$ in front of the symmetric Ch$O(4)$ term grows rapidly with increasing temperature the soliton becomes unstable already at relatively low temperatures below 100 MeV. This unphysical phenomenon is due to the Lagrangian (2.1) restricted to Ch$O(\leqslant 4)$; with explicit σ mesons there appears no such difficulty.

For our further discussion we will therefore choose the minimal renormalization scheme (ii) with temperature-independent ℓ_i's. The corresponding renormalization group (RG) equations [12–14] for the parameters f and m of the NLS model are written in differential form

$$df^2 = -2\frac{\partial g_1}{\partial T}dT = -2(dg_1 + g_2 dm^2), \tag{3.1}$$

$$d(f^2m^2) = -\tfrac{3}{2}m^2\frac{\partial g_1}{\partial T}dT = -\tfrac{3}{2}m^2(dg_1 + g_2 dm^2).$$

These equations, augmented by the corresponding expression for the vacuum partition function (2.5),

$$d\left(\frac{\ln Z_{\rm vac}}{\beta V}\right) = \frac{3}{2}\frac{\partial g_0}{\partial T}dT \tag{3.2}$$

$$= d(f^2m^2) + \tfrac{3}{2}d(g_0 + m^2 g_1) + \tfrac{3}{2}m^2 g_2 dm^2$$

are solved numerically. In order to obtain an analytical solution which can be compared to ChPT the terms proportional to dm^2 may be neglected. Because dm^2 is at least Ch$O(4)$ [see Eq. (3.3) below] these terms contribute to the action only at Ch$O(\geqslant 6)$ where many other contributions are also omitted. On the other hand by solving the RG equations in this way we sum up a class of diagrams to *all* chiral orders: these are just the chain, daisy, and superdaisy graphs [15] as will be noticed immediately. The solution, where quantities evaluated at $T=0$ are marked by the subscript zero, is

$$f^2 = f_0^2 - 2g_1(m,T),$$

$$m^2 = m_0^2\left[1 - \frac{2g_1(m,T)}{f_0^2}\right]^{-1/4}, \tag{3.3}$$

$$\frac{\ln Z_{\rm vac}}{\beta V} = f^2m^2 + \frac{3}{2}[g_0(m,T) + m^2 g_1(m,T)].$$

These expressions, exact in the chiral limit, were checked against the numerical solution of the RG equations (3.1), (3.2): there are only marginal deviations at higher temperatures. The parameters f and m are plotted in Fig. 1. If Eq. (3.3) is systematically expanded to Ch$O(8)$

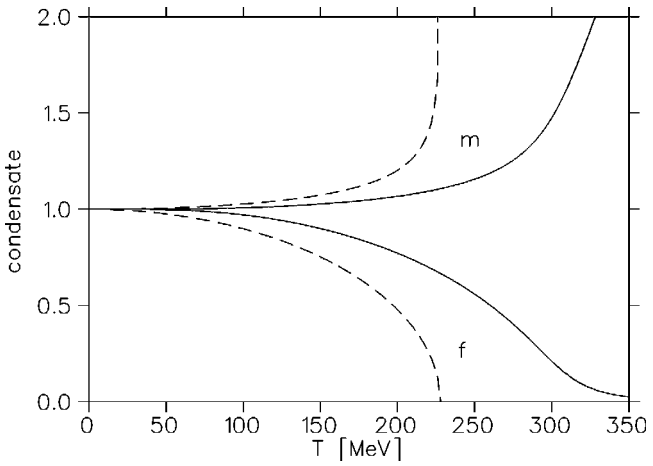

FIG. 1. Temperature dependence of the pion decay constant f and the pion mass m as derived from the RG equation (full lines). In the chiral limit (dashed lines) the pion decay constant vanishes and the pion mass diverges at the critical temperature. All quantities in this and the following figures are plotted relative to their values at $T=0$.

$$\frac{\ln Z_{\rm vac}}{\beta V} = f_0^2m_0^2 + \tfrac{3}{2}g_0(m_0,T) + \frac{3m_0^2g_1^2(m_0,T)}{8f_0^2} + \frac{m_0^2g_1^2(m_0,T)}{16f_0^2}[5g_1(m_0,T) - 3m_0^2g_2(m_0,T)] + \cdots, \tag{3.4}$$

the ChPT result of [16] is reproduced except for part of one diagram of Ch$O(8)$ which is not of the chain or daisy type. Although the RG improvement is meant to extend the one-loop results to higher temperatures and although the relations (3.3) describe a second order chiral phase transition (subsequent subsection) we have to be cautious: because the model does not explicitly include heavier mesons such as vector mesons and especially the scalar meson which plays a crucial role in chiral symmetry restoration the results may not be trusted close to the phase transition, e.g., the critical temperature turns out to be much too high here.

A. Vacuum sector

All thermodynamical properties of the vacuum are derived from the partition function $Z_{\rm vac}$ (3.3). Examples are the free and internal vacuum energy densities

$$F_{\rm vac}/V \equiv -\frac{\ln Z_{\rm vac}}{\beta V} = -\tfrac{3}{2}[g_0(m,T) + m^2g_1(m,T)] - f^2m^2,$$

$$U_{\rm vac}/V \equiv -\frac{\partial \ln Z_{\rm vac}}{V\partial\beta} = +\tfrac{3}{2}[3g_0(m,T) + m^2g_1(m,T)] - f^2m^2, \tag{3.5}$$

and the quark condensate. The quark condensate is obtained as a derivative with respect to the quark mass $m_q \sim m_0^2$:

$$\langle \overline{q}q\rangle \equiv -\frac{\partial}{\partial m_q}\left(\frac{\ln Z_{\rm vac}}{\beta V}\right) = \frac{\langle \overline{q}q\rangle_0}{f_0^2}\frac{\partial}{\partial m_0^2}\left(\frac{\ln Z_{\rm vac}}{\beta V}\right),$$

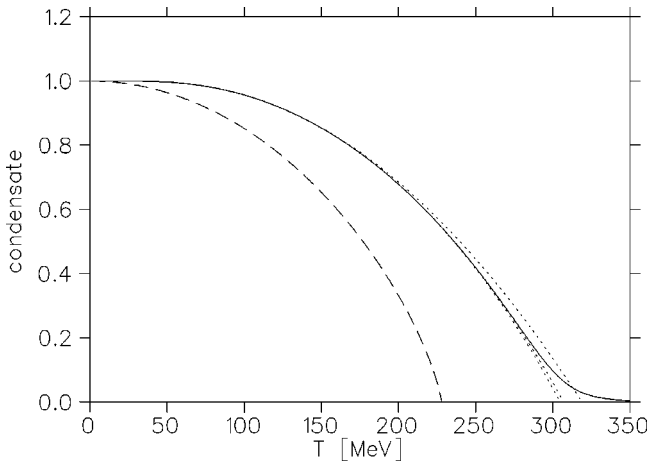

FIG. 2. Temperature dependence of the quark condensate as derived from the RG equation (full line). In the chiral limit (dashed line) the quark condensate vanishes at the critical temperature. For comparison the one-, two- and three-loop ChPT results are also depicted (dotted lines).

$$\langle \overline{q}q\rangle = \langle \overline{q}q\rangle_0 \frac{f^2m^2}{f_0^2m_0^2} = \langle \overline{q}q\rangle_0 \left[1-\frac{2g_1(m,T)}{f_0^2}\right]^{3/4}.$$

The relation $\langle \overline{q}q\rangle \sim f^2m^2$, which should hold for a consistent RG scheme at finite temperature, follows here from the definition after some nontrivial algebra using Eq. (3.3). The quark condensate is compared with one-, two-, and three-loop ChPT results [16] in Fig. 2. The pion mass and the quark condensate scale with the pion decay constant as

$$m \sim f^{-1/4}, \quad \langle \overline{q}q\rangle \sim f^{3/2}, \tag{3.6}$$

which, although rigorous at low temperatures, is not meant to remain valid close to the phase transition for the reasons already discussed.

Nevertheless we briefly comment on the chiral limit $m_0 \to 0$ where the expressions (3.3), (3.5), (3.6) simplify (dashed lines in Figs. 1 and 2) and on the chiral phase transition

$$f^2 \underset{m_0\to 0}{\sim} f_0^2\left[1-\frac{T^2}{6f_0^2}\right], \quad m^2 \underset{m_0\to 0}{\sim} m_0^2\left[1-\frac{T^2}{6f_0^2}\right]^{-1/4},$$

$$F_{\rm vac}/V \underset{m_0\to 0}{\sim} -\frac{\pi^2}{30}T^4, \quad U_{\rm vac}/V \underset{m_0\to 0}{\sim} +\frac{\pi^2}{10}T^4, \tag{3.7}$$

$$\langle \overline{q}q\rangle \underset{m_0\to 0}{\sim} \langle \overline{q}q\rangle_0\left[1-\frac{T^2}{6f_0^2}\right]^{3/4}.$$

Pion decay constant f, quark condensate $\langle \overline{q}q\rangle$, and the gluon condensate $f^4/8(\ell_1+\ell_2)$ become zero at the same critical temperature $T_c=\sqrt{6}f_0$. The diverging pion mass and the too large critical temperature are artifacts of the missing heavier mesons, in particular, the σ meson. Critical exponents according to the standard definitions (specific heat $C \equiv -Td^2F_{\rm vac}/dT^2$)

$$C \underset{m_q\to 0}{\sim} |T-T_c|^{\alpha}, \quad \langle \overline{q}q\rangle \underset{m_q\to 0}{\sim} |T-T_c|^{\beta},$$

$$\frac{\partial\langle \overline{q}q\rangle}{\partial m_q} \underset{m_q\to 0}{\sim} |T-T_c|^{-\gamma}, \quad \langle \overline{q}q\rangle \underset{T=T_c}{\sim} m_q^{1/\delta} \tag{3.8}$$

are readily read off: $\alpha=0$, $\beta=\frac{3}{4}, \gamma=\frac{3}{8}, \delta=3$. At least the coefficients α, β, and δ agree with the leading terms of an ε expansion [17] [$\gamma=\frac{3}{8}$ instead of $\gamma=\frac{1}{2}$ suffers from the approximation leading to Eq. (3.3)]. However, they deviate substantially from those of the $O(4)$ Heisenberg magnet obtained in the *linear* σ model [18,19]. A smooth connection of the low-temperature behavior of all these quantities as discussed here with the linear σ model results at the critical temperature T_c is highly desirable. A simple Padé approximation [20,21] which connects the two temperature regions cannot be the solution to this problem.

B. Soliton sector

Via the temperature dependence of f and m the soliton in tree approximation is now itself temperature dependent and so are the fluctuations and the phase shifts. In the end $\ln Z/Z_{\rm vac}$ (2.5) is given by the temperature-dependent soliton mass plus the Casimir energy (2.13), but now without the term $2\pi a_1 g_1$ which is already taken care of by the RG equation. The Casimir energy must not be forgotten: it destroys the scaling behavior of the tree approximation and brings the results back close to those of the one-loop calculation (Sec. II). The results for the free and internal soliton energies as well as the axial-vector coupling constant and the pion-nucleon coupling are shown in Figs. 3 and 4. The temperature dependence of the nucleon mass turns out to be modest (compared to that of the pion decay constant f). The coupling constants tend to decrease with increasing temperature. There are other quantities such as the σ term and the electric polarizability which show a much more pronounced temperature-dependence. The σ term plotted in Fig. 5 melts very quickly with increasing temperature. The RG result starts to deviate from one-loop at relatively low tempera-

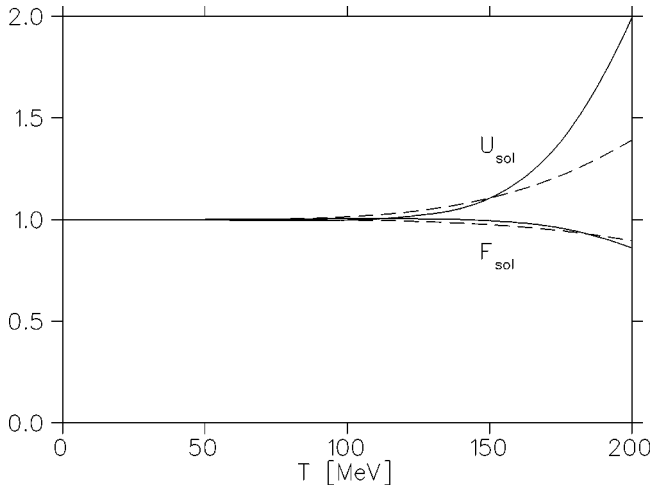

FIG. 3. Temperature dependence of the free soliton energy $F_{\rm sol}$ and the internal soliton energy $U_{\rm sol}$. The one-loop calculations (dashed) are compared to the RG results (solid).

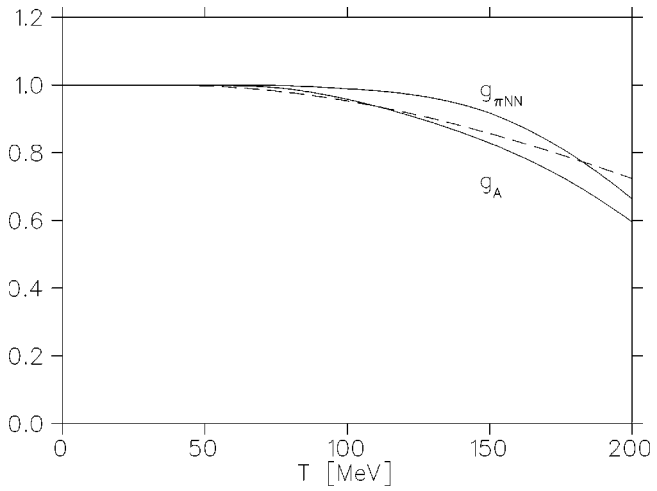

FIG. 4. Temperature dependence of the axial-vector coupling g_A and the pion-nucleon coupling $g_{\pi NN}$. The one-loop calculations (dashed) are compared to the RG results (solid).

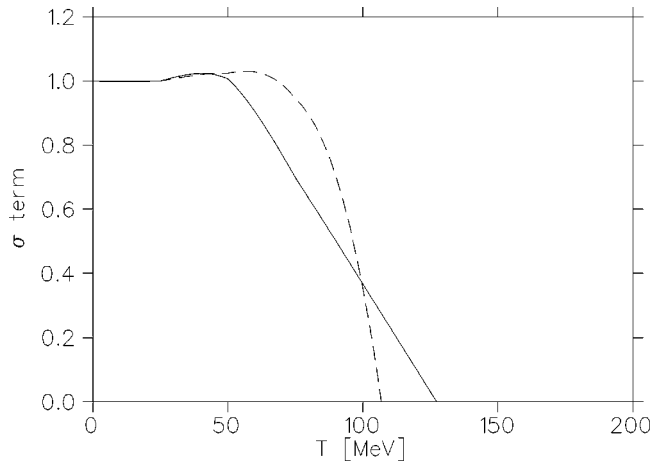

FIG. 5. Temperature dependence of the σ term. The one-loop calculation (dashed) is compared to the RG result (solid).

tures, obviously higher loops are much more important for this quantity as compared to the soliton energies and coupling constants already discussed. For the electric polarizability (not plotted) there is the opposite finding: it increases rapidly with increasing temperature. However, it seems questionable whether these observables can be measured in a hot environment.

IV. CONCLUSION

The chiral soliton model is quite suitable for the study of the nucleon in the heat bath of hot pions because it contains both ingredients which are necessary: the pions and the nucleon as chiral soliton in one and the same model. The temperature-dependence of baryon properties enters via the one-loop contribution. For the most important quantities determining the behavior of hot nucleonic matter this leads to an almost constant mass and to a modestly decreasing pion-nucleon coupling in the low-temperature regime.

In order to implement the temperature dependence already on the tree level (temperature-dependent soliton) the finite temperature RG equations are studied. These comprise and extend the well-established ChPT results for the temperature-dependent pion decay constant, pion mass, and chiral quark condensate. There is no need to lend these quantities from other models. Via these temperature-dependent parameters the soliton is now itself temperature dependent, however, the remaining one-loop contribution cannot be disregarded. If this contribution is taken properly into account, the nucleon mass and the axial-vector coupling are again back close to the naive one-loop result. For other quantities, such as, e.g., the σ term and the electric polarizability, which show a much more pronounced temperature dependence, the RG treatment deviates from the naive one-loop result with increasing temperature indicating the importance of higher loop effects. Unfortunately these quantities are hardly experimentally accessible in a hot environment.

No simple scaling law was found in this investigation. The scaling hypothesis relies on the tree approximation and the one-loop contribution destroys this behavior. If we allow for temperature-dependent Ch$O(4)$ LEC's according to the maximal renormalization scheme, in particular for a temperature-dependent Skyrme parameter e, the scaling behavior is improved but still far from being satisfactory. This is caused by the higher chiral order terms contained in one-loop which are important in the soliton sector.

The RG improvement presented here extends the rigorous ChPT results to higher temperatures and leads to a second order phase transition. Nevertheless, the validity of this investigation remains limited to the low temperature region because of serious shortcomings of the underlying model. To extend the procedure towards the phase transition a RG treatment which includes heavier mesons, in particular the σ meson, has to be developed. At present, there is not even a RG scheme which connects the ChPT results in the low-temperature region smoothly with the $O(4)$ symmetry expected in the linear σ model at critical temperature. More than that, quark degrees of freedom which cannot be treated within the framework of effective Lagrangians may certainly become important close to the phase transition [22].

ACKNOWLEDGMENTS

I have benefited from numerous discussions with G. Holzwarth, H. Geyer, and S. Marculescu.

[1] V. L. Eletsky and I. I. Kogan, Phys. Rev. D **49**, R3083 (1994).
[2] V. Bernard and U.-G. Meissner, Ann. Phys. (N.Y.) **206**, 50 (1991).
[3] J. Gasser and H. Leutwyler, Phys. Lett. B **184**, 83 (1987).
[4] V. Bernard, U.-G. Meissner, and I. Zahed, Phys. Rev. D **36**, 819 (1987).
[5] G. E. Brown and M. Rho, Phys. Rev. Lett. **66**, 2720 (1991).
[6] J. Gasser and H. Leutwyler, Ann. Phys. (N.Y.) **158**, 142

(1984): Nucl. Phys. **B250**, 465 (1985).
[7] F. Meier and H. Walliser, Phys. Rep. (to be published).
[8] B. Schwesinger, J. Weigel, G. Holzwarth, and A. Hayashi, Phys. Rep. **173**, 173 (1989).
[9] B. Moussallam, Ann. Phys. (N.Y.) **225**, 284 (1993).
[10] H. Leutwyler and A. V. Smilga, Nucl. Phys. **B342**, 302 (1990).
[11] M. Kacir and I. Zahed, Phys. Rev. D **54**, 5536 (1996).
[12] H. Matsumoto, Y. Nakano, and H. Umezawa, Phys. Rev. D **29**, 1116 (1984).
[13] Y. Fujimoto, K. Ideura, Y. Nakano, and H. Yoneyama, Phys. Lett. **167B**, 406 (1986).
[14] P. Elmfors, Z. Phys. C **56**, 601 (1992).
[15] H. Nakkagawa and H. Yokota, Mod. Phys. Lett. A **11**, 2259 (1996).
[16] P. Gerber and H. Leutwyler, Nucl. Phys. **B321**, 387 (1989).
[17] J. Zinn-Justin, *Quantum Field Theory and Critical Phenomena* (Clarendon, Oxford, 1989). The ε expansion ($d=2+\varepsilon$, $\varepsilon=1$) to $O(\varepsilon^0)$ in the NLS model leads to critical exponents $\alpha=0, \beta=\frac{3}{4}, \gamma=\frac{1}{2}, \delta=3$.
[18] F. Wilczek, Int. J. Mod. Phys. A **7**, 3911 (1992).
[19] K. Rajagopal and F. Wilczek, Nucl. Phys. **B399**, 395 (1993).
[20] A. Bochkarev and J. Kapusta, Phys. Rev. D **54**, 4066 (1996).
[21] S. Jeon and J. Kapusta, Phys. Rev. D **54**, 6475 (1996).
[22] A. Kocić and J. Kogut, Nucl. Phys. **B455**, 229 (1995).